Available online at www.sciencedirect.com
SCIENCE DIRECT®
Molecular Immunology 42 (2005) 125–136
Molecular Immunology
www.elsevier.com/locate/molimm

Molecular characterization of a panel of murine monoclonal antibodies specific for the SARS-coronavirus

Michael J. Gubbins[a], Frank A. Plummer[a,b], Xin Y. Yuan[a], Darrell Johnstone[a], Mike Drebot[a,b], Maya Andonova[a], Anton Andonov[a,b], Jody D. Berry[b,c,*]

[a] *National Microbiology Laboratory, Health Canada, 1015 Arlington Street, Winnipeg, Man., Canada R3E 3R2*
[b] *Department of Medical Microbiology, University of Manitoba, Basic Medical Sciences Building, 730 William Avenue, Winnipeg, Man., Canada R3E 0W3*
[c] *National Center for Foreign Animal Disease, Canadian Food Inspection Agency, 1015 Arlington Street, Winnipeg, Man., Canada R3E 3M4*

Received 11 May 2004; accepted 9 June 2004
Available online 9 August 2004

Abstract

The availability of monoclonal antibodies (mAbs) specific for the SARS-coronavirus (SARS-CoV) is important for the development of both diagnostic tools and treatment of infection. A molecular characterization of nine monoclonal antibodies raised in immune mice, using highly purified, inactivated SARS-CoV as the inoculating antigen, is presented in this report. These antibodies are specific for numerous viral protein targets, and six of them are able to effectively neutralize SARS-CoV in vitro, including one with a neutralizing titre of 0.075 nM. A phylogenetic analysis of the heavy and light chain sequences reveals that the mAbs share considerable homology. The majority of the heavy chains belong to a single Ig germline V-gene family, while considerably more sequence variation is evident in the light chain sequences. These analyses demonstrate that neutralization ability can be correlated with specific murine V_H-gene alleles. For instance, one evident trend is high sequence conservation in the V_H chains of the neutralizing mAbs, particularly in CDR-1 and CDR-2. The results suggest that optimization of murine mAbs for neutralization of SARS-CoV infection will likely be possible, and will aid in the development of diagnostic tools and passive treatments for SARS-CoV infection.

Keywords: Immunogenetics; Monoclonal antibody; Murine; Neutralizing; Phylogenetic analysis; SARS-coronavirus

1. Introduction

SARS-coronavirus (SARS-CoV), the causative agent of severe acute respiratory syndrome (SARS) in humans, has infected more than 8000 people in various countries worldwide and caused approximately 800 deaths (Drosten et al., 2003a,b; WHO; http://www.who.int/csr/sars/country/en/). The whole genomes of SARS-CoV isolates, implicated in the 2003 outbreak in Toronto, have been sequenced and characterized (Marra et al., 2003; Rota et al., 2003). Characterization of this virus continues at a phenomenal rate, and our understanding of the function of numerous viral proteins, the phylogeny of SARS-CoV, and the viral life cycle continues to grow (reviewed in Stadler et al., 2004; Eickmann et al., 2003; Thiel et al., 2003).

Currently, no effective vaccines or treatments for SARS-CoV infection are available. Until an effective vaccine is developed, the best hope for the treatment of infection and the

Abbreviations: CDR, complementarity determining region; CoV, coronavirus; D, diversity; F.C.A., Freund's complete adjuvant; F.I.A., Freund's incomplete adjuvant; FR, framework; Ig, immunoglobulin; I.P., intraperitoneal; J, joining; PBS, phosphate buffered saline; SARS, severe acute respiratory syndrome; S.C., subcutaneous; V_H, variable region heavy chain; V_L, variable region light chain

* Corresponding author. Present address: The Monoclonal Antibody Section, NCFAD/NML, 1015 Arlington Street, Winnipeg, Man., Canada R3E 3M4. Tel.: +1 204 789 6063; fax: +1 204 789 2038
E-mail address: berryjd@inspection.gc.ca (J.D. Berry).

0161-5890/$ – see front matter © 2004 Elsevier Ltd. All rights reserved.
doi:10.1016/j.molimm.2004.06.032

prevention and control of future outbreaks remains the development of passive immunotherapy with SARS-CoV-specific antibodies (Holmes, 2003). It has been suggested that protection might be afforded by passive immunotherapy with concentrated SARS-CoV-specific IgG antibodies (Li et al., 2003a), and reports have established that infected individuals can benefit from treatment with serum from recovered patients (Pearson et al., 2003). Recently, it was also reported that viral replication was inhibited in the lower respiratory tract of naïve mice if they underwent passive immunization with neutralizing antibodies present in immune serum derived from infected mice (Subbarao et al., 2004). A monoclonal antibody developed from a human non-immune single chain variable region (scFv) library has also been shown to neutralize SARS-CoV in vitro, strengthening the argument that passive immunotherapy with highly specific mAbs might be very effective in controlling SARS-CoV infection (Sui et al., 2004).

The production of mAbs specific for SARS-CoV is vital for studies of viral pathogenesis, and the development of both diagnostic tools and vaccines. Since the development of serum antibodies after infection with SARS-CoV can take 1–3 weeks (Li et al., 2003a), assays that can accurately detect the presence of viral nucleic acids or proteins may be preferred for rapid diagnosis of SARS-CoV infection. The profiles of antibody responses to SARS-CoV have been well established (Li et al., 2003a). Analyses have also identified viral proteins that might serve as the best markers for immunological detection of infection by SARS-CoV (Tan et al., 2004; Lu et al., 2004). Similarly, the characterization of immunogenic peptides derived from SARS-CoV structural proteins has also allowed for the identification of epitopes that are recognized by antibodies present in patient serum (Wang et al., 2003). With this knowledge, the development of mAbs that can be used for both diagnostic assays and clinical treatments should be an attainable goal.

Herein, we further characterize the immunogenetics and neutralizing endpoints of purified murine hybridoma-derived mAbs raised in mice, using highly purified SARS-CoV as the inoculating antigen. Numerous reports exist, which characterize antibodies raised against surrogate SARS-CoV immunogens. Examples include polyclonal antibodies raised against peptides and a recombinant SARS-CoV nucleoprotein (Chang et al., 2004; Lin et al., 2003), and monoclonal antibodies raised against a SARS-CoV-derived recombinant protein fragment (Zhou et al., 2004). Similarly, a neutralizing mAb specific for the spike protein, derived from naïve human phage display libraries, has been developed and characterized (Sui et al., 2004). Little has been published on mAbs developed to the native viral particle. The relevant immunogenetic characteristics of a panel of nine murine mAbs raised to whole SARS-CoV, six of which can effectively neutralize the virus in vitro, are presented. This development provides a distinct advantage in the search for an effective passive immune therapy, because these mAbs were raised against the intact virus, rather than any individual viral protein or immunogenic peptide.

2. Materials and methods

2.1. Production of highly purified SARS-CoV for inoculation of mice

All of the procedures employed for the production of SARS-CoV are discussed in detail in Berry et al. (2004). Briefly, SARS-CoV (Tor-3 strain; Krokhin et al., 2003) was expanded after plaque purification in Vero-6 cell monolayers and partially purified through a sucrose cushion, and then further purified using iodixanol gradient centrifugation. Fractions were tested by Western immunoblot with convalescent patient serum, and the fractions that reacted with SARS-CoV were pooled, dialyzed against phosphate buffered saline (PBS), and further concentrated by ultracentrifugation for 1.5 h at 150,000 × *g*, resulting in highly purified whole virus particles.

2.2. Inoculation of mice and production of hybridomas and antibodies

All of the procedures employed for the production of hybridomas and mAbs are discussed in detail in Berry et al. (2004). Briefly, 5–6-week-old female BALB/c mice (Charles River, Wilmington, MA) were injected subcutaneous (S.C.) with 50 μg of beta-propiolactone-inactivated SARS-CoV (Tor-3 strain) with an equal part of Freund's complete adjuvant (F.C.A.) (H37-Ra) from Difco (BD, Oakville, ON). Thirty days later, the mice received 50 μg of SARS-CoV S.C. in Freund's incomplete adjuvant (F.I.A.) in a total volume of 100 μl. The mice received 5 μg of the same antigen in a total volume of 100 μl S.C. with F.I.A. on days 48 and 63. The mice received a final booster inoculation intraperitoneal (I.P.) with 5 μg of highly purified SARS-CoV in 200 μl PBS 3 days before euthanization by anesthesia overdose, spleen removal, and subsequent hybridoma fusion. After hybridoma fusion and establishment of stable clones, the hybridoma supernatants were screened via ELISA using purified SARS-CoV as the target antigen, and isotyped with a commercial murine isotyping dipstick test (Roche), facilitating the selection of appropriate primers for subsequent RT-PCR. Monoclonal antibodies were produced in medium scale in 450 and 800 cm^2 sterile disposable roller bottle flasks (Corning). Roller bottles containing 200 ml of complete hybridoma media [BD-Quantum yield (VWR, Canada), 10% fetal bovine serum (Wisent, Montreal), 10% Biogro-Hybridoma serum-free supplement (Biogro Technology, Winnipeg)] were inoculated with 50 ml of hybridoma cells such that a final concentration of more than 1 million viable cells/ml was achieved. The cultures were allowed to grow to extinction and were harvested at 7–10 days post-inoculation. Supernatants were clarified

by removing cell mass by centrifugation, and concentrated on Amicon 8400 stirred cell Ultrafiltration-nitrogen concentrators (VWR, Canada) with a YM-30 (Millipore, USA) membrane. Individual membranes were used for the concentration of each mAb. The concentrated supernatants were mixed 1:1 with protein A-binding buffer (Pierce) and purified on a equilibrated 1 or 5 ml protein G-sepharose column (Amersham Biotech) as per the manufacturers instructions. Eluted antibody was dialyzed to remove salt using Centriprep YM-30 Centrifugal Filter Units (Millipore) with a 30 kDa cutoff. The mAb solutions were filter sterilized through low-protein-binding 0.22 μm syringe filters (VWR). Protein concentration was determined using the micro-bca assay (Pierce) and the IgG concentration was standardized to 1 mg/ml in sterile PBS (Gibco).

2.3. Virus neutralization assay

The SARS-CoV in vitro neutralization assay was performed essentially as described (Berry et al., 2004), with the following modifications. The panel of purified mAbs was sterile filtered and each sample standardized to a concentration of 1 mg/ml of IgG before being subjected to serial dilutions and incubation with live SARS-CoV.

2.4. Cloning of the heavy (V_H) and light (V_L) chains of murine mAbs

Approximately 1–2 million mAb-secreting hybridoma cells were collected and homogenized via passage through a 20-guage needle using an RNase-free 5 ml syringe. Total RNA was isolated using RNeasy® Mini Spin kit according to the manufacturer's instructions (QIAGEN®). cDNA was produced via reverse transcription using 10 pg to 10 μg of RNA template, a 15 base oligo-dT primer and SuperScript II reverse transcriptase (Invitrogen). Reactions were incubated at 42 °C for 1 h, followed by inactivation of the reverse transcriptase at 70 °C for 15 min. RNA was removed from the reactions by incubating them with RNaseH (Invitrogen) at 37 °C for 20 min. The resulting cDNA was used as a template for PCR amplification using Taq polymerase (Invitrogen) and various 5′ and 3′ primers specific for V_H and V_L genes and. The primers used are as follows (in 5′–3′ orientation), and are described in detail elsewhere (Berry, 1999; Barbas et al., 2001; Dattamajumdar et al., 1996). V_H-specific, 5′: UmIgVH: TGA GGT GCA GCT GGA GGA GTC; MHCL-1: ATG GAC TTB GDA YTG AGC T; MHCL-2: ATG GAA TGG ASC TGG RTC TTT CTC T; MHCL-3: ATG AAA GTG TTG AGT CTG TTG TAC GTG; MHCL-4: ATG RAS TTS KGG YTM ARC TKG RTT; MHC9: AGG TII AIC TIC TCG AGT CWG G; MSCVH-9: GGT GGT TCC TCT AGA TCT TCC CTC GAG GTG AWG YTG GTG GAG TC; MSCVH-10: GGT GGT TCC TCT AGA TCT GCC CTC GAG GTG CAG SKG GTG GAG TC. V_H-specific, 3′: MH125: GGC CAG TGG ATA GAC. V_L-specific, 5′: MVL: GTG CCA GAT GTG AGC TCG TGA TGA CCC AGT CTC CA; MSCVK-9: GGG CCC AGG CGG CCG AGC TCG AYA TTG TTC TAC WCC AGT C; MSCVK-10: GGG CCC AGG CGG CCG AGC TCG AYA TTG WGC TSA CCC AAT C. V_L-specific, 3′: MCK-1: GGA TAC AGT TGG TGC AGC. Degenerate nucleotides are indicated as follows: B = T, C, or G; D = A, T, or G; I = deoxyinosine; K = T or G; M = A or C; R = A or G; S = C or G; W = A or T; Y = C or T. PCR reactions were incubated at 94 °C for 2 min, followed by 30 cycles of 96 °C for 15 s, 56 °C for 30 s, and 72 °C for 2 min. A final extension at 72 °C for 10 min completed the reactions. Approximately 1–5 μg of the PCR products were resolved on 2% agarose gels and stained with ethidium bromide. PCR products of the appropriate size (350–500 base-pairs) were inserted into the Invitrogen pCR2.1-TOPO-TA™ vector and transformed into TOP-10 cells, according to the manufacturer's instructions. Colonies containing the plasmid with insert were selected by overnight growth, at 37 °C, on Luria–Bertani agar plates containing ampicillin (200 μg/ml) and X-gal (80 μg/ml). White (positive) colonies were incubated in 5 ml of Luria–Bertani broth containing ampicillin (200 μg/ml) for 12–16 h with vigorous shaking at 37 °C, and plasmids were isolated using QIAprep® Spin Miniprep DNA isolation kits, according to the manufacturer's instructions (QIAGEN®). *Eco*RI digestion of 1–5 μg of the resulting plasmids and resolution of the products via agarose gel electrophoresis, as described above, confirmed the presence of the appropriately sized inserts. One to 10 putative positive clones were sequenced with T7 (5′-TAA TAC GAC TCA CTA TAG GG-3′) and M13Rev (5′-CAG GAA ACA GCT ATG AC-3′) primers, using ABI Prism® BigDye™ terminator cycle sequencing kits and an ABI Prism® 3100 Genetic Analyzer. Consensus sequences were generated using the DNASTAR software suite (DNASTAR Inc.). GenBank accession numbers are AY605265 to AY605273 for the V_H sequences, and AY605274 to AY605282 for the V_L sequences presented in this work.

2.5. Identification of Ig germline sequences and assignment of relevant regions

Consensus nucleotide sequences were compared against the *Mus musculus* immunoglobulin (Ig) set database using IMGT/V-Quest (Lefranc, 2003; http://imgt.cines.fr/home.html). The sequences were concurrently compared against the *M. musculus* Ig germline V-gene database using IgBlast (Altschul et al., 1990; http://www.ncbi.nlm.nih.gov/igblast/). This allowed the identification of the complementarity determining region (CDR) and framework (FR) regions of the V_H and V_L sequences, and provided numbering to the inferred amino acid sequences according to Kabat et al. (1991). Similarly, the IgBlast results allowed for the identification of the most closely related murine Ig germline V-genes currently available in these databases. In all cases, the entire sequence, including those at the 5′ end of each sequence imposed by the specific primers used in the original PCR amplification, were examined.

2.6. Sequence alignments

The inferred amino acid sequences were trimmed to remove all residues encoded by the 5′ primer regions, to eliminate potential artefactual matches caused by the primers employed in PCR amplification of the heavy and light chains. The sequences were then aligned with ClustalW (Thompson et al., 1994; http://clustalw.genome.ad.jp/) using standard parameters (gap open penalty: 10; gap extension penalty: 0.05; no weight transition; hydrophilic gaps allowed; weight matrix: Blosum). The alignments were then analyzed using GeneDoc version 2.6.002 (Nicholas et al., 1997) to produce textual alignments and quantify the relatedness of the sequences.

2.7. Phylogenetic analysis

Analyses were performed using BioEdit version 5.0.9 (Hall, 1999) and MEGA version 2.1 software suite (Kumar et al., 2001). Only amino acid sequences were examined. The sequences, aligned via ClustalW as described above, were analyzed via neighbor joining analysis, bootstrapped using 1000 replicates. The naïve human mAb 80R (Sui et al., 2004; V_H GenBank accession no. AAS19425; V_L GenBank accession no. AAS19432) was initially used as an outlier sequence. This mAb was chosen because it is specific for the SARS-CoV spike protein and neutralizes SARS infection in vitro, but it was developed from a non-immune human single chain variable fragment (scFv) library. A second outlier, also human in origin, was found as follows. The V_L and V_H amino acid sequences of F26G18 were compared against the human Ig sequences in the NCBI databases using IgBlast, as described above. F26G18 was chosen because it was the most potent SARS neutralizing murine mAb isolated, and it is specific for spike. Human antibodies were chosen to ensure that similarity would be minimal, considering that mouse, and indeed human, antibodies inherently share considerable homology regardless of their specificity. The sequences that showed the lowest homology to the V_H and V_L sequences of F26G18 were chosen as follows: V_L: GenBank accession no. BAC01727, level of identity: 83/115 amino acids; V_H: GenBank accession no. CAD19025, level of identity: 83/132 amino acids. In all of the phylogenetic analyses, the human sequences clearly served as effective outliers, and only BAC01727 and CAD19025 are included in the relevant figures.

3. Results

3.1. Summary of the relevant genetic properties of the mAbs specific for SARS-CoV

Table 1 summarizes the relevant characteristics of the murine mAbs generated against highly purified, inactivated SARS-CoV. Examining the V_H chains, only two Ig V-gene

Table 1
Summary of relevant properties of the V_H and V_L regions of murine mAbs specific for SARS-CoV

mAb[a]	Class	GenBank accession numbers	Target[b]	Neutralizing titre (nM)	J-gene[c]	D-gene[c]	Most closely related Ig germline V-gene[d]	Percent identity to most closely related Ig germline V-gene[e]	
								Nucleotide	Amino acid
V_H									
F26G1	G2a/k	AY605271	Spike	–	J_H4	SP2.6/7/8	VOx-1	92	85
F26G6	G2b/k	AY605272	Spike	–	J_H2	None	J558.33	95	89
F26G8	G2a/k	AY605273	Spike	–	J_H2	None	J558.33	95	86
F26G18	G2b/k	AY605269	Spike	0.075	J_H4	FL16.2	J558.50	97	91
F26G19	G2a/k	AY605270	Spike	1	J_H4	Q52.01	J558.50	97	89
F26G3	G2a/k	AY605265	U	26	J_H1	FL16.1	J558.5	96	94
F26G7	G2b/k	AY605266	U	6	J_H4	Q52.01	J558.50	97	91
F26G9	G2a/k	AY605267	U	1	J_H1	SP2.3/4/5	J558.50	97	94
F26G10	G2a/k	AY605268	U	1	J_H1	SP2.3/4/5	J558.50	96	91
V_L									
F26G1	G2a/k	AY605280	Spike	–	J_k2	N.A.	ay4	99	96
F26G6	G2b/k	AY605281	Spike	–	J_k4	N.A.	bw20	94	86
F26G8	G2a/k	AY605282	Spike	–	J_k4	N.A.	bw20	92	81
F26G18	G2b/k	AY605278	Spike	0.075	J_k2	N.A.	ce9	97	92
F26G19	G2a/k	AY605279	Spike	1	J_k1	N.A.	cw9	98	96
F26G3	G2a/k	AY605274	U	26	J_k2	N.A.	21-7	98	92
F26G7	G2b/k	AY605275	U	6	J_k1	N.A.	cw9	98	95
F26G9	G2a/k	AY605276	U	1	J_k2	N.A.	19-25	98	94
F26G10	G2a/k	AY605277	U	1	J_k2	N.A.	19-25	99	98

[a] Neutralizing mAbs are indicated by bold text.
[b] U: unknown.
[c] Most closely related genes, as determined by V-quest and NCBI IgBlast analysis of nucleotide sequences. N.A.: not applicable.
[d] As determined by NCBI IgBlast analysis of nucleotide sequences.
[e] Expressed as percentage of identical residues (pairwise), as determined by NCBI IgBlast of nucleotide or inferred amino acid sequences, as indicated.

(A)

```
J558.50: TGGGACTGTGCTGGCAGGGCCTGGGGCTTCAGTGAAGATGTCCTGCAAGGCTTCTGGCTACACCTTTACCAGCTACTGGATGCACTGGGTAAAACAGAGGCCTGGACAGGGTCTGGAATGGATTGGC
 F26G18: .........T..C..A.....................................................................................................................: 127
 F26G19: ..............A.....................................................C....C...........A.....................................: 127
 F26G7 : A.............A.....................................G.....................C.............A.....................................: 127
 F26G9 : ..............A.............C.....................................G.....................................................A..........T : 127
 F26G10: ..............A.............C.....................................G.....................................................A..T........T : 127

J558.50: GCTATTTATCCTGGAAATAGTGATACTAGCTACAACCAGAAGTTCAAGGGCAAGGCCAAACTGACTGCAGTCACATCCACCAGCACTGCCTACATGGAGCTCAGCAGCCTGACAAATGAGGACTCTG
 F26G18: ............................A.....................G.....C.............................C.....................................: 254
 F26G19: ............................C.....................A.....................................T.....................................: 254
 F26G7 : ...........A.................C.....................................................................................................: 254
 F26G9 : ...........................................................................G....T.....................................: 254
 F26G10: ...........A.....................................................................G.....................A.....................: 254

J558.50: CGGTCTATTACTGTACAAGA
 F26G18: .................... : 274
 F26G19: .........T.......... : 274
 F26G7 : .................... : 274
 F26G9 : .................... : 274
 F26G10: .................... : 274
```

(B)

```
                FR1                CDR-1     FR2              CDR-2                FR3
J558.50: SGTVLAGPGASVKMSCKASGYTFT  SYWMH  WVKQRPGQGLEWIG  AIYPGNSDTSYNQKFKG  KAKLTAVTSTSTAYMELSSLTNEDSAVYYCTR
 F26G18: .....PR.................  .....  ..............  .........N.......  R.T.........S.................. : 92
 F26G19: ......R.................  T.R..  .I............  .........T......D  ...........S..............F... : 92
 F26G7 : ......R.........E.......  T....  .I............  .........T.......  ............................... : 92
 F26G9 : ......R..............S..  .....  ..............  ...............  .........A..................... : 92
 F26G10: ......R..............S..  .....  ..........D...  ....E............  .........A......H.............. : 92
```

Fig. 1. Alignments of the nucleotide and amino acid sequences of V_H regions of the neutralizing mAbs belonging to the J558 V-gene family. (A) Nucleotide alignment of the V_H regions of the mAbs most closely related to the J558.50 V-gene. The consensus sequence used is that of J558.50 (nucleotide sequence GenBank accession no. AF303881). A dot in the individual sequences denotes nucleotides that are the same as the consensus. A dash in the individual sequences denotes a deletion. Neutralizing clones are shown in bold text. (B) Amino acid alignment of the V_H regions of the mAbs most closely related to the J558.50 Ig V-gene. The consensus sequence used is that of J558.50 (amino acid sequence GenBank accession no. AAG39162). A dot in the individual sequences denotes amino acids that are the same as the consensus. A dash in the individual sequences denotes a deletion. The framework and complementarity determining regions (CDR) are indicated above the appropriate sequence segments in the figure.

families are represented. Eight out of the nine mAbs share high sequence identity with the J558 V-gene family, with the remaining mAb, F26G1, sharing high sequence identity with the VOx-1 gene. Of the J558 V-gene family members, five of the eight mAbs are most closely related to the J558.50 V-gene, and this set of five mAbs neutralizes SARS-CoV in vitro. mAbs F26G6, F26G8 and F26G3 are most closely related to the J558.33 and J558.5 V-genes, respectively, which are themselves closely related to J558.50. A closer analysis of the V_H chains of mAbs sharing significant homology with the J558.50 V-gene is presented in Fig. 1 and Table 2. An alignment of the nucleotide sequences of these V_H sequences reveals a very high level of identity (Fig. 1A). Similarly, at the amino acid level, these sequences share considerable identity both amongst themselves and with the J558.50 V-gene (Fig. 1B), with some mutation away from the germline sequence, which is typical of immunoglobulin V-gene cDNAs from T-dependant B cell responses (Fish and Manser, 1987). A quantification of the level of identity of these sequences is summarized in Table 2. An analysis of the J-genes shows that three J_H genes are represented in the V_H chains, at a relatively even distribution. There appears to be a slight bias towards J_H4 (four mAbs) with J_H1 (three mAbs) and J_H2 (two mAbs) also represented (Table 1). Analysis of the CDR-3 sequences reveals that D_H-regions are present in seven out of nine of the mAbs, with homology to numerous D_H-gene sequences available in the databases. A detailed analysis of the D_H-regions is presented in the following section.

Table 2
Comparison of the V_H regions of the SARS-CoV-specific neutralizing mAbs sharing significant homology with the J558.50 Ig germline V-gene

mAb	Level of identity vs. J558.50	
	Nucleotide	Amino acid
F26G18	267/274 (97%)	86/92 (93%)
F26G19	266/274 (97%)	84/92 (91%)
F26G7	267/274 (97%)	87/92 (95%)
F26G9	267/274 (97%)	89/92 (97%)
F26G10	265/274 (97%)	86/92 (93%)

Level of identity (pairwise) is expressed as number of identical residues/total number of residues and percent identical residues.

Examination of the V_L chains demonstrates that a wider variety of V-genes is represented. Six distinct V-genes are present, which suggests that a larger pool of V-genes can be selected, compared to the V_H chains, to produce mAbs that are specific for SARS-CoV. As in the case for V_H, three J-gene families are represented, with a definite bias towards J_k2 (five mAbs) and an even distribution of J_k1 and J_k4 (two mAbs each).

3.2. Analysis of the V_H and V_L sequences of the mAb panel

An alignment of all of the amino acid sequences of the V_H and V_L chains is presented in Fig. 2A. An inspection of the V_H sequences reveals that CDR-1 and CDR-2 share a relatively high level of identity in all of the mAbs. Conversely, CDR-3 shows a considerably higher level of sequence variation. A close inspection of the V_H sequences shows that F26G6/F26G8, F26G7/F26G19, and F26G9/F26G10 are all

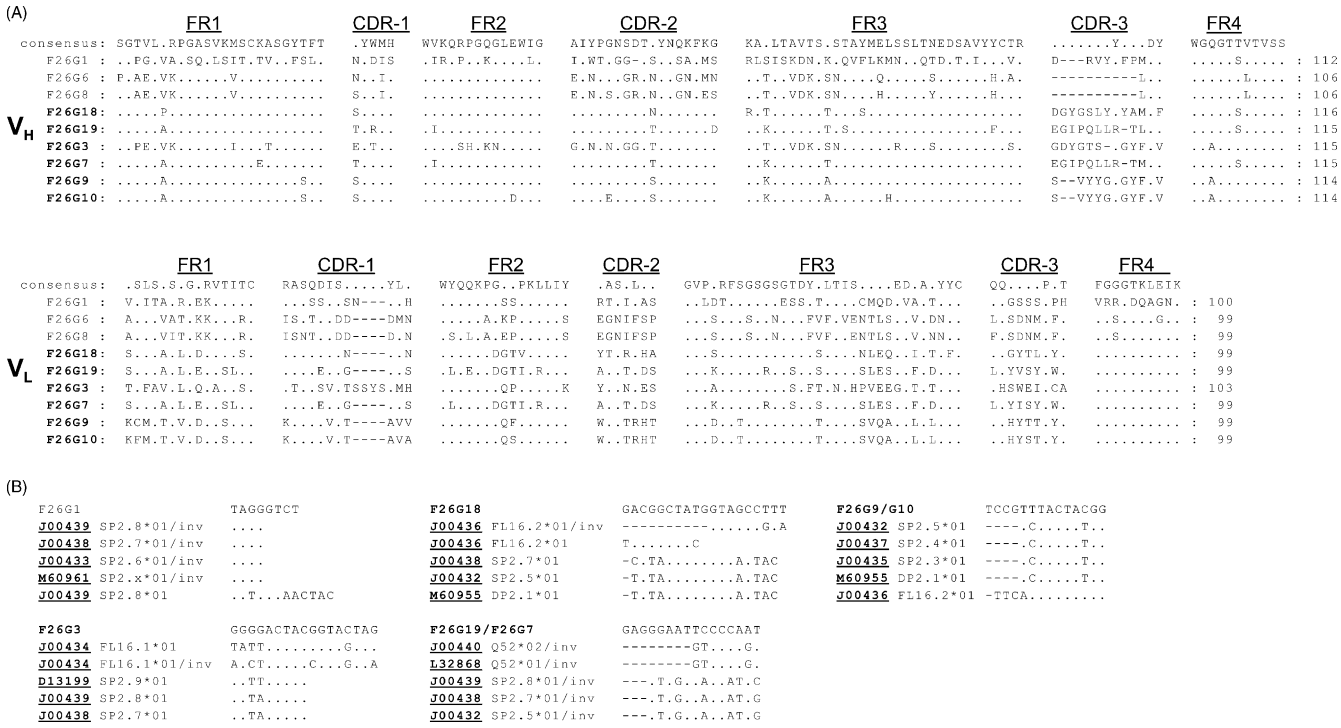

Fig. 2. (A) Amino acid alignment of the V_H and V_L regions of the murine mAbs raised against SARS-CoV. The consensus sequence (top line) shows amino acid residues that are conserved in >50% of the sequences. A dot in the consensus sequence denotes amino acids that are conserved in <50% of the listed sequences. A dot in the individual sequences denotes amino acids that are the same as the consensus. A dash in the individual sequences denotes a deletion. Neutralizing mAbs are shown in bold text. The framework (FR) and complementarity determining regions (CDR) are indicated above the appropriate sequences in the figure. (B) Nucleotide alignments of identifiable D-regions in the V_H CDR3 regions. The most closely related D-regions were determined by V-quest analysis as outlined in Section 2. Dots represent identical residues, while dashes represent gaps or nucleotides that were not taken into account for the alignments. Neutralizing mAbs are shown in bold text.

closely related (within each pair), with very few amino acid changes evident between these sequences.

An examination of the V_L sequences reveals that unlike the case of V_H, CDR-1, -2, and -3 exhibit considerably higher levels of sequence variation. As is the case for the V_H chains, the V_L chains of the F26G6/F26G8, F26G7/F26G19, and F26G9/F26G10 pairs share a high level of sequence identity (within each pair) and are therefore likely clonally related. In the case of both the V_H and V_L sequences, mAb F26G1 stands out as being the least closely related to any of the other sequences in this panel of mAbs. A quantitative analysis of sequence relatedness is discussed in the subsequent sections.

The discernible D_H-regions present in the CDR-3 of the V_H domains show considerable variation, and alignments of these regions with available related D_H-region sequences identified by V-quest analysis are shown in Fig. 2B. mAb F26G1 contains the most well delineated but shortest D_H-region, with high homology to SP2.6/7/8 D_H-genes over six nucleotides. mAb F26G3 shows high homology to FL16.1 and considerable homology with SP2.7/8/9 D_H-genes, which also overlaps with FL16.1. mAbs F26G7 and F26G19 contain identical D_H-regions, which share homology with both SP2.5/7/8 and Q52.01/02, although delineation of the regions of homology is less clear. Similarly, mAbs F26G9 and F26G10 contain identical D_H-regions, with homology to SP2.3/4/5, DP2.1, and FL16.2. Manual alignment of the sequences suggests that the central portion of the D_H region of F26G18 is most likely encoded by an SP2 or DP2 element, with considerable junctional diversity (D) on either end (Fig. 2B). mAb F26G18 contains a D_H-region with homology to SP2.5/7, DP2.1, and FL16.2. Discernable D_H-regions are lacking in mAbs F26G6 and F26G8, and these mAbs are therefore not included in this figure. It is clear from the analysis that the D_H-regions of all of these mAbs are highly variable, and likely resulted from complex somatic gene rearrangements and junctional diversification during assembly.

3.3. Quantitative analysis of the relatedness of the regions encoded within the V_H and V_L chains

Examining the full length of the V_H sequences, as outlined in Fig. 2A, a clear pattern emerges regarding amino acid sequence identity. The most closely related V_H sequences are F26G9/F26G10 (97% identical), F26G7/F26G19 (95% identical), F26G6/F26G8 (92% identical) and F26G18/F26G19 (82% identical). Both V_H CDR-1 and CDR-2 exhibit high levels of identity, with all of the neutralizing mAbs showing remarkable sequence conservation, while V_H CDR-3 shows a high level of sequence diversity. One neutralizing mAb F26G3 shares little identity with any of the other neutralizing mAbs because it is derived from a different germline V_H allele (see the following section for a more detailed analysis

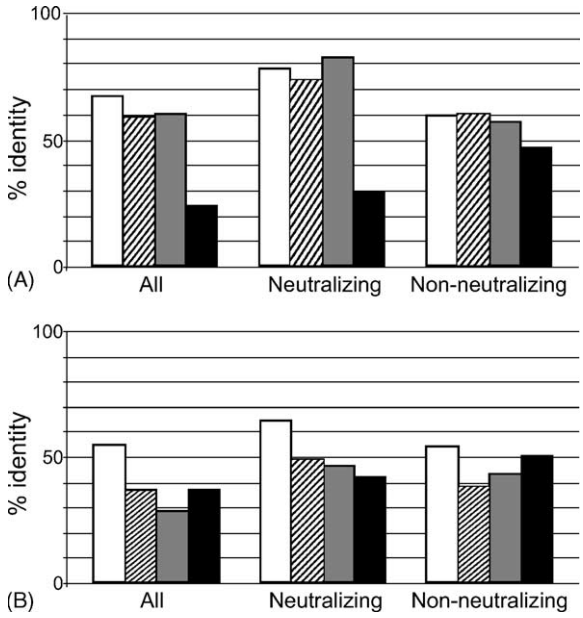

Fig. 3. Summary of the percentage identity of the SARS-CoV-specific mAbs. (A) Summary of the percentage of pairwise identity, at the amino acid level (*Y*-axis), between the V_H chains of various categories of mAbs (all, neutralizing, non-neutralizing) as indicated on the *X*-axis. White bars: full length of sequences; hatched bars: CDR-1; grey bars: CDR-2; black bars: CDR-3. (B) Summary of the percentage of identity at the amino acid level of the V_L sequences. This figure is labeled the same as (A).

of this mAb). The most closely related V_L sequences are F26G7/F26G19 (98% identical), F26G9/F26G10 (96% identical), and F26G6/F26G8 (90% identical). The V_L CDRs exhibit more sequence variability than those found in the V_H chains, and as was the case for F26G3 V_H, the V_L chain of this mAb shows very little sequence identity with the V_L chains of the other neutralizing mAbs (Fig. 2A). For both the V_L and V_H chains, mAb F26G1 demonstrates the lowest sequence identity compared to any of the other mAbs in the panel (Fig. 2A and B).

The average level of identity of the heavy and light chains, subdivided into pertinent regions, is shown in Fig. 3. Across the full length of V_H, it is evident that the average level of identity is highest amongst the neutralizing mAbs, albeit by a small margin (Fig. 3A). An examination of the V_H CDRs reveals that CDR-1 and CDR-2 exhibit the highest level of sequence identity, whether subdivided into groups containing all mAbs, neutralizing mAbs, or non-neutralizing mAbs. However, this finding is most apparent when examining the neutralizing mAbs, whose CDR-1 and CDR-2 regions share 73% and 82% average sequence identity, respectively. On the other hand, CDR-3 exhibits the highest sequence variability, whether grouped into all mAbs, neutralizing mAbs, or non-neutralizing mAbs, with an average level of identity ranging from 24% to 47%. An extended CDR-3 domain is characteristic of the V_H chains of the SARS-CoV neutralizing mAbs. This domain of the neutralizing mAbs contains, on an average, 12 amino acid residues, while the average amongst all of the mAbs is 10 residues (not including D-element negative clones F26G6 and G8). The CDR-3 regions of the non-neutralizing mAbs contain only five residues. The V_L regions exhibit a lower average level of sequence identity, as outlined in Fig. 3B. As with the V_H sequences, the highest average level of identity across the full length of the V_L sequences is exhibited by the neutralizing mAbs. However, the average level of sequence identity is lower overall in the V_L sequences than in the corresponding V_H sequences (Fig. 2A and compare Fig. 3A and B). Unlike the V_H sequences, there is no clear bias towards a higher level of identity in the CDRs, with all three CDRs sharing relatively low average sequence identity, regardless of the grouping of the mAbs into all, neutralizing, or non-neutralizing categories. This finding again suggests that the V_L CDRs likely influence the neutralization ability of the mAbs to a lesser extent than the V_H CDRs.

3.4. Summary of the phylogenetic relationship of the mAbs

The overall relatedness of the V_H and V_L sequences of the mAbs can be quickly summarized via phylogenetic neighbor joining analysis. Fig. 4 shows phylogenetic trees generated by an examination of the amino acid sequences of the V_H and V_L chains. Fig. 4A summarizes the V_H chains. Clearly, the neutralizing mAbs F26G7, F26G9, F26G10, F26G18, and F26G19 cluster together and are closely related. Amongst these V_H chains, F26G18 is the least closely related to the remaining members of this group. Interestingly, F26G18 and F26G19, which are both spike-specific neutralizing mAbs, cluster further apart, and are in fact on separate branches of the tree. Another neutralizing mAb, F26G3, clusters closer to mAbs F26G6 and F26G8, which are non-neutralizing, spike-specific mAbs. Unfortunately, the protein target of mAb F26G3 is currently unknown. However, one would not be surprised if this mAb does in fact target spike, but this interaction has been undetectable by the methods employed thus far (Berry et al., 2004).

Although these analyses cannot determine whether F26G6/F26G8, F26G7/F26G19, and F26G9/F26G10 are in fact mAbs derived from the same clones, it is clear that they cluster in related branches according to their overall properties (e.g. neutralizing, spike-specific). It is also clear that mAb F26G1 is least related to any of the other mAbs in this panel, occupying its own branch well separated from the rest of the mAbs. Examining the V_H chains sharing the highest identity with the J558.50 V-gene, all of which are neutralizing, it is evident that a similar pattern emerges. Monoclonal antibodies F26G9/F26G10 and F26G7/F26G19 are encoded by V-genes that cluster closely together, with F26G18 occupying a divergent branch on the tree (Fig. 4B). Essentially the same pattern emerges when examining the V_L chains (Fig. 4C), with neutralizing and spike-specific mAbs clustering in related branches, and F26G1 occupying a separate branch on the tree, illustrating that this mAb is the least related to any of the other mAbs in the panel.

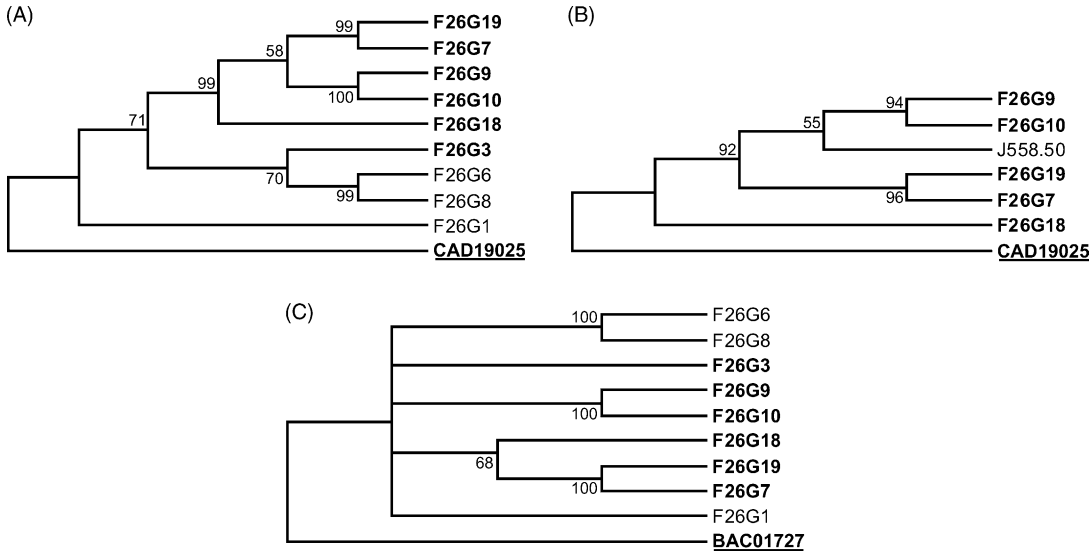

Fig. 4. Phylogenetic analysis of the mAbs specific for SARS-CoV. Trees are based on neighbor joining analysis of the inferred amino acid sequences of the relevant V_H and V_L sequences, as outlined in Section 2. (A) V_H regions of all mAbs. (B) V_H regions of all mAbs sharing significant identity with the J558.50 Ig germline V-gene. (C) V_L regions of all mAbs. In each case, the outliner sequences are of human origin, chosen as outlined in Section 2. Neutralizing mAbs are shown in bold text. The number at each node represents the level of bootstrap support (expressed as a percentage) for the node over the total number of replicates performed. Only those values above 50% are reported.

3.5. Detailed analysis of the neutralizing mAbs

Table 3 presents a summary of the level of identity evident in the group of mAbs that exhibit SARS-CoV neutralizing ability, relative to the most efficiently neutralizing mAb, F26G18. As shown in this table, the neutralizing titre varies from a low of 0.075 nM (F26G18) to a high almost 350-fold greater, at 26 nM (F26G3). As a comparison, it was recently reported that a human mAb, 80R, developed from a naïve human immune scFv library and specific for the angiotensin-converting enzyme 2 (ACE2) binding domain of spike, exhibited a neutralizing concentration as low as 0.37 nM (Sui et al., 2004). The relationship between F26G18 and the rest of the neutralizing mAbs was therefore examined as an attempt to identify any common theme or relationship that exists amongst them. Clearly, mAb F26G3 is least related to F26G18 or any of the other neutralizing mAbs, in both the V_H and V_L chains (Table 3). Examining the V_H chains, the average level of identity (compared to F26G18) for all of the neutralizing mAbs is high across the entire sequence of the

Table 3
Comparison of the V_H and V_L regions of the most efficiently neutralizing mAb (F26G18) with the corresponding regions of the remainder of the neutralizing mAbs

mAb	Neutralizing titre (nM)	Region examined and level of identity vs. F26G18[a]			
		Full length	CDR-1	CDR-2	CDR-3
V_H					
F26G19	1	95/116 (82%)	3/5 (60%)	15/17 (88%)	3/13 (23%)
F26G9	1	96/116 (83%)	5/5 (100%)	16/17 (94%)	2/13 (15%)
F26G10	1	93/116 (80%)	5/5 (100%)	15/17 (88%)	2/13 (15%)
F26G7	6	99/116 (93%)	4/5 (80%)	16/17 (94%)	4/13 (31%)
F26G3	26	77/116 (66%)	3/5 (60%)	11/17 (64%)	4/13 (31%)
Average identity[b] (%)		81 ± 10	80 ± 20	86 ± 12	23 ± 8
V_L					
F26G19	1	69/99 (70%)	8/11 (72%)	2/7 (28%)	3/9 (33%)
F26G9	1	65/99 (66%)	5/11 (45%)	2/7 (28%)	7/9 (77%)
F26G10	1	64/99 (65%)	5/11 (63%)	2/7 (28%)	6/9 (66%)
F26G7	6	70/99 (71%)	8/11 (72%)	2/7 (28%)	3/9 (33%)
F26G3	26	59/103 (57%)	5/15 (33%)	3/7 (42%)	2/9 (22%)
Average identity[b] (%)		66 ± 6	57 ± 17	31 ± 6	46 ± 24

[a] Level of identity (pairwise) is expressed as number of identical residues/total number of residues and percent identical residues. F26G18 is the most efficiently neutralizing mAb, with a neutralizing titre of 0.075 nM.

[b] The average level of identity (±S.D.) is calculated from the values of the specified regions for each given mAb.

V_H chain, and within CDR-1 and CDR-2. Conversely, CDR-3 is the least closely related region in all of the neutralizing mAbs. The same pattern is evident when the average level of sequence identity of the V_H chains across all mAb sequences is examined (Fig. 3A). Examining the V_L chains, the average level of identity between the rest of the neutralizing mAbs and F26G18 is relatively low (Table 3), which is similar to the relatively low average level of identity exhibited by all of the mAbs in the panel (Fig. 3B). The average level of identity in CDR-1 and CDR-2 of V_L is lower, compared to F26G18, than the corresponding regions in V_H, while CDR-3 exhibits a higher average level of identity. In the V_L chains, a slightly lower average level of identity is evident in CDR-2, compared to CDR-1 and CDR-3; however, this is far less noticeable than the difference in relatedness between CDR-3 compared to CDR-1 and CDR-2 in the V_H chains.

4. Discussion and conclusions

This panel of mAbs derived from mice immunized with highly purified whole SARS-CoV exhibits diverse specificity for binding targets and variable in vitro neutralization ability. Neutralization titres amongst the mAbs vary from the lowest, at 0.075 nM for F26G18, to a high of 26 nM, for F26G3. Interestingly, two of the mAbs that exhibit the highest neutralizing efficiency, F26G18 and F26G19, are specific for the spike protein (Berry et al., 2004). As has been established conclusively, spike is required for binding of SARS-CoV to its receptor, ACE2, and mAbs that block this interaction can neutralize SARS-CoV (Li et al., 2003b; Sui et al., 2004). These results suggest that F26G18 and F26G19 likely neutralize SARS-CoV infection by directly targeting spike, although whether the interaction between spike and its receptor is targeted specifically remains to be determined, and ongoing work to answer this question is in progress. Although five of the mAbs are confirmed to be spike-specific, three of these (F26G1, F26G6, and F26G8) are unable to neutralize SARS-CoV infection in vitro. These results suggest that this panel of mAbs recognizes a diverse set of epitopes within the spike protein, some of which are in regions of spike that are not involved in viral adhesion or other steps in the infection process. Of the panel of six neutralizing mAbs, the targets of four have not yet been identified, and work is currently underway to determine them.

Examining the level of pairwise identity of the neutralizing mAbs at the amino acid level reveals that the highest sequence variability is exhibited by the V_H CDR-3, while, not surprisingly, CDR-1 and CDR-2 of the V_H chains demonstrate a greater level of sequence identity. Conversely, all three CDRs of the V_L chains exhibit similar levels of sequence identity, which are, on average, lower than the levels of identity in the corresponding V_H regions. The variability in CDR-3 of the V_H chains is therefore likely a significant contributing factor to the target specificity of these mAbs, and the V_L CDRs likely influence the neutralization ability of the mAbs to a lesser extent than the V_H CDRs. The average length of CDR-3 also appears to influence neutralizing ability. The V_H CDR-3 of the neutralizing mAbs contains more amino acids than the average number in the whole panel of mAbs, while the CDR-3 regions of the non-neutralizing mAbs contain fewer residues. Conversely, the average length of V_L CDR-3 is constant. These results suggest that both the length and sequence of the V_H CDR-3 influence the neutralization ability of the mAbs, most likely by determining the specificity of contact residues for key neutralizing epitopes on SARS-CoV proteins.

Within the group of neutralizing mAbs, a trend is evident that relates homology in the V_H chains of the most potent neutralizing mAb, F26G18, with those that neutralize SARS-CoV less efficiently. The clustering of the sequences of the neutralizing mAbs based on their relatedness to F26G18 tends to correlate well with their ability to neutralize SARS-CoV in vitro. For both V_H and V_L, the mAb with the lowest neutralizing efficiency, F26G3, has the lowest overall sequence identity when compared to mAb F26G18, and when compared to the average sequence identity across the whole panel of neutralizing mAbs. This trend is more apparent for the V_H sequences, since the percentage of identity of the V_L chains relative to F26G18 is lower overall. This observation is consistent with the dominant role of V_H compared to V_L in previously identified neutralizing mAbs against a viral pathogen (Barbas et al., 1993). CDR-1 and CDR-2 of the V_H chains of the neutralizing mAbs are most closely related to the same regions in F26G18, while CDR-3 is less conserved. From this analysis, one can infer that high homology in V_H CDR-1 and CDR-2 (relative to F26G18) of the neutralizing mAbs appears to correlate with neutralizing ability. Interestingly, F26G7 exhibits a six-fold higher neutralizing titre than F26G19, even though their sequences are closely related both to each other and to F26G18, revealing that the trend for relatedness to F26G18 correlating with neutralizing ability does not follow for all of the mAbs in this panel. This observation also suggests that small changes in the amino acid composition of these mAbs can significantly alter neutralization efficiency. Overall, this analysis clearly demonstrates that the V_H regions of the neutralizing mAbs are more highly related than the V_L chains, and suggests that the sequence of the V_L chains plays a smaller role in neutralizing ability than the V_H chains.

Analysis of the sequences of the mAbs reveals that the V_H and V_L chains of several mAbs are closely related. The pairs F26G6/F26G8, F26G7/F26G19, and F26G9/G10 exhibit few differences at the amino acid level, within each pair. This observation could be explained in several ways. First, each pair might have originated from the same B cell progenitor and they are clonally related (Fish et al., 1989), with the few observed sequence variations resulting from somatic mutation. Second, identical CDR-3 rearrangements might have occurred in the B cell progenitors, and antigen selection may have produced several independently rearranged but closely related B cell clones. Third and alternatively,

sequence changes might have occurred during reverse transcription or PCR amplification, and the mAbs originated from the same, independently picked hybridoma clone. While these analyses do not allow a differentiation between these potential causes of this high sequence similarity, we would speculate that the first explanation is most likely true.

The V_H chains of eight of the mAbs belong to the J558 V-gene family, and six of these mAbs neutralize SARS-CoV in vitro. This result suggests that a small pool of B cells, expressing related Ig V-genes, was selected for in response to exposure to SARS-CoV. This is not entirely surprising, considering that the J558 V-gene family is estimated to contain several hundred members in the genome of the BALB/c mouse (Livant et al., 1986) and this family is highly selected in murine B cells (Haines et al., 2001). It is clear that a restricted pool of V_H genes was selected to encode SARS-CoV neutralizing mAbs. A bias towards the selection of genes in the J558 V-gene family to generate autoantibodies in the tight-skin mouse has also been reported (Kasturi et al., 1994). J_H gene usage is distributed relatively evenly in the mAbs generated during this work, which agrees well with the observation that J_H gene usage in several murine innate antibodies belonging to the J558 V-gene family, is approximately evenly distributed (Seidl et al., 1999). These results suggest that a typical variety of joining (J) genes is selected during the generation of V_H chains in these clones. Conversely, a bias was evident in the selection of J genes in the generation of the V_L chains in these clones, which agrees with published reports of preferential selection of J_k1 and J_k2 genes in adult mouse splenic cells (Wood and Coleclough, 1984; Nishi et al., 1985). This observation suggests that the V_L chains of these mAbs appear to be derived from a more diverse pool of V genes, and may be less critical for contributing contact residues, relative to V_H, for binding to SARS-CoV proteins. A complete absence of D_H-regions, and as a result a small CDR-3 in the V-domain, in two of the non-neutralizing, spike-specific mAbs, F26G6 and F26G8, suggests that this region contributes significantly to neutralization. The diversity of the length, sequences, and apparent order of assembly of the D_H-regions present in these mAbs suggests that significant somatic alteration of sequences flanking the D_H-regions occurred during junctional assembly, or that somatic mutations occurred during affinity maturation in a germinal center. The presence of identical D_H elements in the CDR-3 regions of F26G7/F26G19 and F26G9/F26G10 supports the notion that these pairs are clonally related, and derived from the same parental V-gene rearrangement.

In summary, multiple mAbs able to neutralize SARS-CoV infection in vitro were generated in this work, and they display neutralization titres in the nanomolar to picomolar range. The majority of the V_H chains of the neutralizing mAbs share significant homology to the J558 Ig V-gene family, suggesting selection of a limited pool of V-genes occurred in mice exposed to highly purified SARS-CoV. High levels of sequence identity in CDR-1 and CDR-2 of the V_H chains, compared to low levels of sequence identity in all of the V_L chains, suggests that neutralization ability is imparted to these mAbs by contact residues within the V_H chains. Chain shuffling experiments will be employed to determine the relative contributions of the V_H and V_L chains to SARS-CoV neutralization (Berry et al., 2003).

Passive immune therapy is a viable treatment for exposure to numerous viruses. The development of the mAbs reported here is an important first step in isolating mAbs generated against the intact SARS virus that could be used for passive immunotherapy. Humanization of murine mAbs is a viable method for the development of potential passive immunotherapeutics (Roguska et al., 1994; Rader et al., 1998), and these methods can be applied to the mAbs developed in this work. One caveat to this analysis is that it is not an exhaustive statistical analysis of the relationships between the mAbs described here. Due to the small numbers of mAbs examined, only trends and general relationships regarding the levels of sequence identity between any of the mAbs and their immunological properties can be inferred. Regardless, this analysis provides a useful summary of murine mAbs that possess the potential for development into viable immune therapies and diagnostic tools for SARS-CoV infection. The recurrent usage of particular murine V-gene elements to encode virus-neutralizing antibodies is becoming more evident and detailed molecular analyses become available (Kalinke et al., 1996). Studies with animal models are currently underway to determine the in vivo neutralization properties of the neutralizing mAbs summarized here.

Acknowledgements

We thank Ms. Allison Land for assistance with the phylogenetic analyses, and staff of the Animal Care Facility at the National Microbiology Laboratory for their expert help. Thanks are also extended to Dr. Paul Kitching, Dr. Raymond Tsang, Dr. Steven Jones, Dr. Amin Kabani, Ms. Brigitte Nicolas, Ms. Fran Ranada and Mr. Tony Saliba, for their valued contributions to this work. This work was funded jointly by Health Canada and the Canadian Food Inspection Agency. M.J.G. is supported by a Health Canada Postdoctoral Fellowship through the Office of the Chief Scientist.

References

Altschul, S.F., Gish, W., Miller, W., Myers, E.W., Lipman, D.J., 1990. Basic local alignment search tool. J. Mol. Biol. 215, 403–410.

Barbas III, C.F., Burton, D.R., Scott, J.K., Silverman, G.J., 2001. Phage Display: A Laboratory Manual. Cold Spring Harbor Laboratory Press, New York.

Barbas III, C.F., Collet, T.A., Amberg, W., Roben, P., Binley, J.M., Hoekstra, D., Cababa, D., Jones, T.M., Williamson, R.A., Pilkington, G.R., Haigwood, N.L., Cabezas, E., Satterthwaite, A.C., Sanz, I., Burton, D.R., 1993. Molecular profile of an antibody response to HIV-1 as probed by combinatorial libraries. J. Mol. Biol. 230, 812–823.

Berry, J.D., 1999. Ph.D. Thesis. The University of Manitoba, Canada.

Berry, J.D., Rutherford, J., Silverman, G.J., Kaul, R., Elia, M., Gobuty, S., Fuller, R., Plummer, F.A., Barbas III, C.F., 2003. Development of functional human monoclonal single-chain variable fragment antibody against HIV-1 from human cervical B cells. Hybrid. Hybridomics 22, 97–108.

Berry, J.D., Jones, S., Drebot, M., Andanov, A., Li, Y., Yang, X., Weingartl, H., Andanov, M., Gubbins, M., Plummer, F., Kabani, A., 2004. Development and characterization of neutralizing monoclonal antibodies to the SARS-coronavirus (hCoV). J. Virol. Methods 120 (1), 87–96.

Chang, M.S., Lu, Y.T., Ho, S.T., Wu, C.C., Wei, T.Y., Chen, C.J., Hsu, Y.T., Chu, P.C., Chen, C.H., Chu, J.M., Jan, Y.L., Hung, C.C., Fan, C.C., Yang, Y.C., 2004. Antibody detection of SARS-CoV spike and nucleocapsid protein. Biochem. Biophys. Res. Commun. 314, 931–936.

Dattamajumdar, A.K., Jacobson, D.P., Hood, L.E., Osman, G.E., 1996. Rapid cloning of any rearranged mouse immunoglobulin variable genes. Immunogenetics 43, 141–151.

Drosten, C., Gunther, S., Preiser, W., van der Werf, S., Brodt, H.R., Becker, S., Rabenau, H., Panning, M., Kolesnikova, L., Fouchier, R.A., Berger, A., Burguiere, A.M., Cinatl, J., Eickmann, M., Escriou, N., Grywna, K., Kramme, S., Manuguerra, J.C., Muller, S., Rickerts, V., Sturmer, M., Vieth, S., Klenk, H.D., Osterhaus, A.D., Schmitz, H., Doerr, H.W., 2003a. Identification of a novel coronavirus in patients with severe acute respiratory syndrome. N. Engl. J. Med. 348, 1967–1976.

Drosten, C., Preiser, W., Gunther, S., Schmitz, H., Doerr, H.W., 2003b. Severe acute respiratory syndrome: identification of the etiological agent. Trends Mol. Med. 9, 325–327.

Eickmann, M., Becker, S., Klenk, H.D., Doerr, H.W., Stadler, K., Censini, S., Guidotti, S., Masignani, V., Scarselli, M., Mora, M., Donati, C., Han, J.H., Song, H.C., Abrignani, S., Covacci, A., Rappuoli, R., 2003. Phylogeny of the SARS coronavirus. Science 302, 1504–1505.

Fish, S., Manser, T., 1987. Influence of the macromolecular form of a B cell epitope on the expression of antibody variable and constant region structure. J. Exp. Med. 166, 711–724.

Fish, S., Zenowich, E., Fleming, M., Manser, T., 1989. Molecular analysis of original antigenic sin. I. Clonal selection, somatic mutation, and isotype switching during a memory B cell response. J. Exp. Med. 170, 1191–1209.

Haines, B.B., Angeles, C.V., Parmelee, A.P., McLean, P.A., Brodeur, P.H., 2001. Germline diversity of the expressed BALB/c VhJ558 gene family. Mol. Immunol. 38, 9–18.

Hall, T.A., 1999. BioEdit: a user friendly biological sequence alignment editor and analysis program for Windows 95/98/NT. Nucleic Acids Symposium Series 41, 95–98.

Holmes, K.V., 2003. SARS coronavirus: a new challenge for prevention and therapy. J. Clin. Invest. 111, 1605–1609.

Kabat, E.A., Wu, T.T., Perry, H.M., Gottesman, K.S., Foeller, C., 1991. Sequences of Proteins of Immunological Interest. U.S. Department of Health and Human Services, Washington, DC, USA.

Kalinke, U., Bucher, E.M., Ernst, B., Oxenius, A., Roost, H.P., Geley, S., Kofler, R., Zinkernagel, R.M., Hengartner, H., 1996. The role of somatic mutation in the generation of the protective humoral immune response against vesicular stomatitis virus. Immunity 5, 639–652.

Kasturi, K.N., Shibata, S., Muryoi, T., Bona, C.A., 1994. Tight-skin mouse: an experimental model for scleroderma. Int. Rev. Immunol. 11, 253–271.

Krokhin, O., Li, Y., Andonov, A., Feldmann, H., Flick, R., Jones, S., Stroeher, U., Bastien, N., Dasuri, K.V., Cheng, K., Simonsen, J.N., Perreault, H., Wilkins, J., Ens, W., Plummer, F., Standing, K.G., 2003. Mass spectrometric characterization of proteins from the SARS virus: a preliminary report. Mol. Cell. Proteomics 2, 346–356.

Kumar, S., Tamura, K., Jakobsen, I.B., Nei, M., 2001. MEGA2: molecular evolutionary genetics analysis software. Bioinformatics 17, 1244–1245.

Lefranc, M.P., 2003. IMGT, the international ImMunoGeneTics database. Nucleic Acids Res. 31, 307–310.

Li, G., Chen, X., Xu, A., 2003a. Profile of specific antibodies to the SARS-associated coronavirus. N. Engl. J. Med. 349, 508–509.

Li, W., Moore, M.J., Vasilieva, N., Sui, J., Wong, S.K., Berne, M.A., Somasundaran, M., Sullivan, J.L., Luzuriaga, K., Greenough, T.C., Choe, H., Farzan, M., 2003b. Angiotensin-converting enzyme 2 is a functional receptor for the SARS coronavirus. Nature 426, 450–454.

Lin, Y., Shen, X., Yang, R.F., Li, Y.X., Ji, Y.Y., He, Y.Y., Shi, M.D., Lu, W., Shi, T.L., Wang, J., Wang, H.X., Jiang, H.L., Shen, J.H., Xie, Y.H., Wang, Y., Pei, G., Shen, B.F., Wu, J.R., Sun, B., 2003. Identification of an epitope of SARS-coronavirus nucleocapsid protein. Cell Res. 13, 141–145.

Livant, D., Blatt, C., Hood, L., 1986. One heavy chain variable region gene segment subfamily in the BALB/c mouse contains 500–1000 or more members. Cell 47, 461–470.

Lu, L., Manopo, I., Leung, B.P., Chng, H.H., Ling, A.E., Chee, L.L., Ooi, E.E., Chan, S.W., Kwang, J., 2004. Immunological characterization of the spike protein of the severe acute respiratory syndrome coronavirus. J. Clin. Microbiol. 42, 1570–1576.

Marra, M.A., Jones, S.J., Astell, C.R., Holt, R.A., Brooks-Wilson, A., Butterfield, Y.S., Khattra, J., Asano, J.K., Barber, S.A., Chan, S.Y., Cloutier, A., Coughlin, S.M., Freeman, D., Girn, N., Griffith, O.L., Leach, S.R., Mayo, M., McDonald, H., Montgomery, S.B., Pandoh, P.K., Petrescu, A.S., Robertson, A.G., Schein, J.E., Siddiqui, A., Smailus, D.E., Stott, J.M., Yang, G.S., Plummer, F., Andonov, A., Artsob, H., Bastien, N., Bernard, K., Booth, T.F., Bowness, D., Czub, M., Drebot, M., Fernando, L., Flick, R., Garbutt, M., Gray, M., Grolla, A., Jones, S., Feldmann, H., Meyers, A., Kabani, A., Li, Y., Normand, S., Stroher, U., Tipples, G.A., Tyler, S., Vogrig, R., Ward, D., Watson, B., Brunham, R.C., Krajden, M., Petric, M., Skowronski, D.M., Upton, C., Roper, R.L., 2003. The genome sequence of the SARS-associated coronavirus. Science 300, 1399–1404.

Nicholas, K.B., Nicholas Jr., H.B., Deerfield II, D.W., 1997. GeneDoc: analysis and visualization of genetic variation. EMBnet. NEWS 4, 14.

Nishi, M., Kataoka, T., Honjo, T., 1985. Preferential rearrangement of the immunoglobulin kappa chain joining region J kappa 1 and J kappa 2 segments in mouse spleen DNA. Proc. Natl. Acad. Sci. USA 82, 6399–6403.

Pearson, H., Clarke, T., Abbott, A., Knight, J., Cyranoski, D., 2003. SARS: what have we learned? Nature 424, 121–126.

Rader, C., Cheresh, D.A., Barbas III, C.F., 1998. A phage display approach for rapid antibody humanization: designed combinatorial V gene libraries. Proc. Natl. Acad. Sci. U.S.A. 95, 8910–8915.

Roguska, M.A., Pedersen, J.T., Keddy, C.A., Henry, A.H., Searle, S.J., Lambert, J.M., Goldmacher, V.S., Blattler, W.A., Rees, A.R., Guild, B.C., 1994. Humanization of murine monoclonal antibodies through variable domain resurfacing. Proc. Natl. Acad. Sci. U.S.A. 91, 969–973.

Rota, P.A., Oberste, M.S., Monroe, S.S., Nix, W.A., Campagnoli, R., Icenogle, J.P., Penaranda, S., Bankamp, B., Maher, K., Chen, M.H., Tong, S., Tamin, A., Lowe, L., Frace, M., DeRisi, J.L., Chen, Q., Wang, D., Erdman, D.D., Peret, T.C., Burns, C., Ksiazek, T.G., Rollin, P.E., Sanchez, A., Liffick, S., Holloway, B., Limor, J., McCaustland, K., Olsen-Rasmussen, M., Fouchier, R., Gunther, S., Osterhaus, A.D., Drosten, C., Pallansch, M.A., Anderson, L.J., Bellini, W.J., 2003. Characterization of a novel coronavirus associated with severe acute respiratory syndrome. Science 300, 1394–1399.

Seidl, K.J., Wilshire, J.A., MacKenzie, J.D., Kantor, A.B., Herzenberg, L.A., Herzenberg, L.A., 1999. Predominant VH genes expressed in innate antibodies are associated with distinctive antigen-binding sites. Proc. Natl. Acad. Sci. U.S.A. 96, 2262–2267.

Stadler, K., Masignani, V., Eickmann, M., Becker, S., Abrignani, S., Klenk, H.D., Rappuoli, R., 2004. SARS-beginning to understand a new virus. Nat. Rev. Microbiol. 1, 209–218.

Subbarao, K., McAuliffe, J., Vogel, L., Fahle, G., Fischer, S., Tatti, K., Packard, M., Shieh, W.J., Zaki, S., Murphy, B., 2004. Prior infection

and passive transfer of neutralizing antibody prevent replication of severe acute respiratory syndrome coronavirus in the respiratory tract of mice. J. Virol. 78, 3572–3577.

Sui, J., Li, W., Murakami, A., Tamin, A., Matthews, L.J., Wong, S.K., Moore, M.J., St. Clair, T.A., Olurinde, M., Choe, H., Anderson, L.J., Bellini, W.J., Farzan, M., Marasco, W.A., 2004. Potent neutralization of severe acute respiratory syndrome (SARS) coronavirus by a human mAb to S1 protein that blocks receptor association. Proc. Natl. Acad. Sci. U.S.A. 101, 2536–2541.

Tan, Y.J., Goh, P.Y., Fielding, B.C., Shen, S., Chou, C.F., Fu, J.L., Leong, H.N., Leo, Y.S., Ooi, E.E., Ling, A.E., Lim, S.G., Hong, W., 2004. Profiles of antibody responses against severe acute respiratory syndrome coronavirus recombinant proteins and their potential use as diagnostic markers. Clin. Diagn. Lab. Immunol. 11, 362–371.

Thiel, V., Ivanov, K.A., Putics, A., Hertzig, T., Schelle, B., Bayer, S., Weissbrich, B., Snijder, E.J., Rabenau, H., Doerr, H.W., Gorbalenya, A.E., Ziebuhr, J., 2003. Mechanisms and enzymes involved in SARS coronavirus genome expression. J. Gen. Virol. 84, 2305–2315.

Thompson, J.D., Higgins, D.G., Gibson, T.J., 1994. CLUSTAL W: improving the sensitivity of progressive multiple sequence alignment through sequence weighting, position-specific gap penalties and weight matrix choice. Nucleic Acids Res. 22, 4673–4680.

Wang, J., Wen, J., Li, J., Yin, J., Zhu, Q., Wang, H., Yang, Y., Qin, E., You, B., Li, W., Li, X., Huang, S., Yang, R., Zhang, X., Yang, L., Zhang, T., Yin, Y., Cui, X., Tang, X., Wang, L., He, B., Ma, L., Lei, T., Zeng, C., Fang, J., Yu, J., Wang, J., Yang, H., West, M.B., Bhatnagar, A., Lu, Y., Xu, N., Liu, S., 2003. Assessment of immunoreactive synthetic peptides from the structural proteins of severe acute respiratory syndrome coronavirus. Clin. Chem. 49, 1989–1996.

Wood, D.L., Coleclough, C., 1984. Different joining region J elements of the murine kappa immunoglobulin light chain locus are used at markedly different frequencies. Proc. Natl. Acad. Sci. U.S.A. 81, 4756–4760.

Zhou, T., Wang, H., Luo, D., Rowe, T., Wang, Z., Hogan, R.J., Qiu, S., Bunzel, R.J., Huang, G., Mishra, V., Voss, T.G., Kimberly, R., Luo, M., 2004. An exposed domain in the Severe Acute Respiratory Syndrome coronavirus spike protein induces neutralizing antibodies. J. Virol. 78, 7217–7226.